HHS Public Access

Author manuscript

Dev Biol. Author manuscript; available in PMC 2018 September 01.

Published in final edited form as:

Dev Biol. 2017 September 01; 429(1): 260–270. doi:10.1016/j.ydbio.2017.06.020.

BmpR1A is a major type 1 BMP receptor for BMP-Smad signaling during skull development

Haichun Pan[1], **Honghao Zhang**[1], **Ponnu Abraham**[1], **Yoshihiro Komatsu**[1,3], **Karen Lyons**[2], **Vesa Kaartinen**[1], and **Yuji Mishina**[1,*]

[1]Department of Biologic & Materials Sciences, School of Dentistry, University Michigan, Ann Arbor, MI 48109, USA

[2]Department of Molecular, Cell and Developmental Biology, University of California, Los Angeles, Los Angeles, CA, USA

[3]Department of Pediatrics, The University of Texas Medical School at Houston, Houston, Texas, USA

Abstract

Craniosynostosis is caused by premature fusion of one or more sutures in an infant skull, resulting in abnormal facial features. The molecular and cellular mechanisms by which genetic mutations cause craniosynostosis are incompletely characterized, and many of the causative genes for diverse types of syndromic craniosynostosis have not yet been identified. We previously demonstrated that augmentation of BMP signaling mediated by a constitutively active BMP type IA receptor (ca-BmpR1A) in neural crest cells (ca1A hereafter) causes craniosynostosis and superimposition of heterozygous null mutation of Bmpr1a rescues premature suture fusion (ca1A;1aH hereafter). In this study, we superimposed heterozygous null mutations of the other two BMP type I receptors, Bmpr1b and Acvr1 (ca1A;1bH and ca1A;AcH respectively hereafter) to further dissect involvement of BMP-Smad signaling. Unlike caA1;1aH, ca1A;1bH and ca1A;AcH did not restore the craniosynostosis phenotypes. In our in vivo study, Smad-dependent BMP signaling was decreased to normal levels in mut;1aH mice. However, BMP receptor-regulated Smads (R-Smads; pSmad1/5/9 hereafter) levels were comparable between ca1A, ca1A;1bH and ca1A;AcH mice, and elevated compared to control mice. Bmpr1a, Bmpr1b and Acvr1 null cells were used to examine potential mechanisms underlying the differences in ability of heterozygosity for Bmpr1a vs. Bmpr1b or Acvr1 to rescue the mut phenotype. pSmad1/5/9 level was undetectable in Bmpr1a homozygous null cells while pSmad1/5/9 levels did not decrease in Bmpr1b or Acvr1 homozygous null cells. Taken together, our study indicates that different levels of expression and subsequent activation of Smad signaling differentially contribute each BMP type I receptor to BMP-Smad

*Corresponding author. Yuji Mishina, Ph.D. Department of Biologic and Materials Sciences, School of Dentistry, University of Michigan, 1011 N. University Ave., Ann Arbor, MI 48109, USA. Tel.: +1 734 763 5579; fax: +1 734 647 2110. mishina@umich.edu.

All authors state that they have no conflicts of interest.

signaling and craniofacial development. These results also suggest differential involvement of each type 1 receptor in pathogenesis of syndromic craniosynostoses.

Keywords

BMP Smad signaling; Bmpr1a; Bmpr1b; Acvr1; Craniosynostosis

Introduction

Craniofacial sutures are actively growing sites supporting the continuous growth of facial and calvarial bones. Premature fusion of sutures leads to craniosynostosis. Occurring in approximately 1 in 2,500 live births, craniosynostosis leads to abnormal growth of calvarial bones, increases pressure inside the skull, which affects vision and in the extreme cases, may affect brain development (Mishina and Snider, 2014; Morriss-Kay and Wilkie, 2005; Snider and Mishina, 2014; Wilkie and Morriss-Kay, 2001). Studies in the past have successfully linked craniosynostosis to more than 20 genetic mutations; however, 70% of observed cases have no known genetic etiology (Lajeunie et al., 1995; Mishina and Snider, 2014; Twigg and Wilkie, 2015; Wilkie et al., 2010; Wilkie and Morriss-Kay, 2001). Therefore, it is necessary for further analysis to uncover genetic and pathophysiological mechanisms for diagnosis and development of treatments.

Bone morphogenetic proteins (BMPs), members of the transforming growth factor-β (TGF-β) super family, play important roles in embryonic development, including craniofacial and calvarial bone development (Ishii et al., 2005; Kim et al., 1998; Liu et al., 2007; Urist, 1965). Activation of BMP signaling is through ligand-induced heterotertrameric complex formation. These complexes include type 1 and type II serine threonine kinase receptors. Heterotetrameric complex formation will thereafter lead to activation of type I receptor kinases, which phosphorylate R-Smads (de Caestecker, 2004; Heldin et al., 1997). Phosphorylated Smads will then accumulate into the nucleus where they function as transcriptional co-regulators. Genetics studies have linked BMP signaling with craniofacial and calvarial bone development. Particularly, our recent work demonstrated that a small increase of BMP-Smad signaling in mouse cranial neural crest leads to pre-mature fusion of the anterior frontal suture, which can be rescued by Bmpr1a heterozygosity (Komatsu et al., 2013).

BMP type I receptors play indispensable roles in transducing BMP signaling. In mammals, each BMP type I receptor has a distinct role during embryogenesis. For example, germ-line knockout of Bmpr1a or Acvr1 leads to embryonic lethality at different stages of gastrulation (Gu et al., 1999; Mishina et al., 1999; Mishina et al., 1995); germ-line knockout of Bmpr1b has no lethal impact during embryogenesis (Baur et al., 2000; Yi et al., 2000). On the other hand, during chondrogenesis, all three types of BMP type I receptors play overlapping roles; double and triple mutations of these receptors show more severe phenotypes in chondrogenesis than the loss of a single BMP type I receptor (Rigueur et al., 2015; Yoon et al., 2005; Yoon et al., 2006). Despite the evidence that all BMP type I receptors are expressed during craniofacial and skull development, there is no knowledge available

regarding how each of them is involved in transducing BMP signaling in these tissues during development. Particularly, it is unknown whether BmpR1B or AcvR1 are involved in regulating BMP signaling in craniosynostosis.

In this current study, we investigated the functions of BMP signaling mediated by each type I receptor during craniofacial development and potential involvement in pathogenesis of craniosynostosis by introducing heterozygous null mutations of each BMP type I receptor to the craniosynostosis model mouse we have reported (Hayano et al., 2015; Komatsu et al., 2013). The in vivo studies to rescue craniosynostosis phenotypes and subsequent in vitro studies to contribute BMP-Smad signaling activity demonstrated that BmpR1A plays distinct and major roles in skull development and in pathogenesis of craniosynostosis.

Materials and Methods

Mouse breeding and isolation of primary osteoblasts

The mouse line carrying the Cre-inducible constitutively active Bmpr1a (ca-Bmpr1a, hereafter) transgene was described previously (Kamiya et al., 2008b; Komatsu et al., 2013). We first crossed Bmpr1a$^{+/-}$ (Mishina et al., 1995), Bmpr1b$^{+/-}$ (Yi et al., 2000) and Acvr1$^{+/-}$ (Mishina et al., 1999) mice with P0-Cre mice (C57BL/6J-Tg(P0-Cre)94Imeg (ID 148) provided by CARD, Kumamoto University, Japan) (Yamauchi et al., 1999) to generate mice Bmpr1a$^{+/-}$;P0-Cre, Bmpr1b$^{+/-}$;P0-Cre and Acvr1$^{+/-}$;P0-Cre mice. Subsequently, these mice were bred with ca-Bmpr1a mice to obtain ca-Bmpr1a;P0- Cre;Bmpr1a$^{+/-}$ (ca1A;1aH, hereafter), ca-Bmpr1a;P0-Cre;Bmpr1b$^{+/-}$ (ca1A;1bH, hereafter) and ca-Bmpr1a;P0-Cre;Acvr1$^{+/-}$ (ca1A;AcH, hereafter) mice. Littermates that did not carry either ca-Bmpr1a or P0-Cre and were wild type for the endogenous type I receptors were used as controls (Cont, hereafter). Littermates that carried ca-Bmpr1a and P0-Cre but were wild type for the endogenous type I receptors were used as mutants (ca1A, hereafter). We interbred Bmpr1b$^{+/-}$ mice to generate homozygous null mutant osteoblasts from newborn calvaria (Mansukhani et al., 2000; Yu et al., 2005). For Bmpr1a and Acvr1, we used the following conditional mutant mice to generate homozygous null osteoblasts: Bmpr1a floxed mice (Mishina et al., 2002), Acvr1 floxed mice (Kaartinen et al., 2004), and Ubiquitin-Cre^{ERT2} mice (No. 008085, The Jackson Laboratory) were intercrossed in order to isolate primary osteoblasts from newborn calvaria of which the genotype was either Bmpr1a$^{fx/-}$;Ubi-Cre^{ERT2};R26R/+ or Acvr1a$^{fx/-}$;Ubi-Cre^{ERT2};R26R/+. Cre activity was induced in culture by adding tamoxifen (100 ng/ml) for 6 days to convert the floxed allele to the Cre-recombined null allele (designated as dE). The degree of Cre-dependent recombination was monitored using the R26R Cre reporter allele (Soriano, 1999), and subsequently quantified by genomic QPCR, directly measuring the deleted exons. All mice were maintained on a mixed 129S6 and C57BL6/J background. They were housed in cages in a 20°C room with a 12-hour light/dark cycle. All animal experiments were performed in accordance with the policy and federal law of judicious use of vertebrate animals as approved by the Institutional Animal Care and Use Committee (IACUC) at the University of Michigan.

Micro-computed tomography (μCT)

Skulls were dissected, cleaned of extra tissue, and fixed with 10% formalin overnight. Whole heads were embedded in 1% agarose, placed in a 19 mm diameter tube, and scanned over their entire length using a micro-CT system (μCT40 Scanco Medical). Scan settings were: voxel size 10 μm, medium resolution, 70 kVp, 114 μA, 0.5 mm AL filter, and integration time 500 ms. Surface images were generated as described previously (Komatsu et al., 2013).

Histology, skeletal staining and picrosirious staining

Tissue fixation and section preparation was performed as described previously (Komatsu et al., 2013). The skulls dissected by postnatal day 9 were decalcified in 14% EDTA solution. Hematoxylin & Eosin and Von Kossa staining were performed according to standard protocols. Cranial bones were stained with alizarin red and alcian blue by a standard method (Hogan, 1994; Komatsu et al., 2013). Picrosirius red staining for sections was performed the standard procedure as described previously (Stern et al., 2012). Samples were observed under a polarized light microscope (Olympus BX51 microscope) and photographed.

Cell apoptosis and proliferation assays, immunohistochemistry

Apoptosis in calvaria at E18.5 stage was evaluated via Terminal deoxynucleotidyl transferase dUTP nick end-labeling (TUNEL) assay according to the instruction of ApopTag Red in Situ Apoptosis Detection Kit (Millipore, #S7165). In brief, frozen sections were subsequently heated in citrate buffer in the water bath for 5 min and then were immersed in 5% Donkey serum for 60 min. Slides were incubated with TUNEL reaction mixture at 37°C, 60min in the dark then incubated in Anti-digoxigenin conjugate rhododamine 30 min. After washing with PBS, slides were mounted with ProLong Gold antifade reagent with 4,6-diamidino-2-phenylindole (DAPI; Invitrogen, #P36931). Sections were examined under a fluorescence microscope (Olympus) with a TRITC set filter and positive cells were counted in the frontal suture and the frontal bone. Statistical analysis was performed using Student's T-test. Significance was accepted at $p<0.05$.

Cell proliferation in E18.5 calvaria was detected via examining presence of Ki67. Slides were incubated with an anti-ki67 antibody (Cell Signaling, #D3D5, 1:500) for overnight at 4°C, and incubated with an anti-rabbit IgG conjugated with Alexa Fluor 488 (Invitrogen, #A-21206, 1:200) for 1h at room temperature. Sections were mounted with ProLong Gold antifade reagent with DAPI; Invitrogen. We counted the number of Ki67 positive cells in the frontal suture and the frontal bones. Statistical analysis was performed using Student's T-test. Significance was accepted at $p<0.05$.

For immunohistochemistry, embryos were fixed in 4% PFA at 4°C for 2 hours, incubated in 30% sucrose/PBS at 4°C overnight, embedded in O.C.T. compound (Sakura Finetek, Tokyo, Japan), and serially sectioned at 10 μm. The following antibodies were used in our study: pSmad1/5/9 (Cell Signaling, #13820, 1:100), and E11/Podoplanin (Santa cruz, #sc-53533, 1:100). The samples were incubated with these primary antibodies at 4°C overnight. Alexa Fluor 488 donkey anti-rabbit IgG (Invitrogen, #A21206, 1:100) for pSmad1/5/9 and Alexa Fluor 488 goat anti-hamster IgG (Invitrogen, #A21110, 1:100) for E11/Podoplanin were

used as secondary antibodies. Sections were mounted with ProLong Gold antifade reagent with DAPI (Invitrogen, #P36935).

RNA extraction and qRT-PCR

Total RNA was isolated from a nasal-frontal bone portion at postnatal day 3 using TRIzol (Invitrogen). cDNA was synthesized using SuperScript II cDNA Synthesis (Invitrogen). PCR probes and Random hexamer primers were from Taqman (Life technologies). Primers were: Bmpr1a: Mm00477650_m1; Bmpr1b: Mm00432117_m1; Acvr1: Mm01331069_m1 and Gapdh: Mm99999915_g1. Data were normalized to Gapdh by 2-ΔΔct method (Livak and Schmittgen, 2001). RT-PCR primers to detect deletion of either Acvr1 exon 5 or exon 7 are 5'-CTCTCGGTGGTGTTTGCAGT-3' and 5'-GGGTTGTTTCCCACATCAAGC-3'.

Genomic real-time quantitative PCR was performed using TaqMan Gene Expression Assays to quantify deletion of Bmpr1a and Acvr1 (Bmpr1a: custom designed TaqMan primer set to detect exon 4 (AI89LJ8_F 5'-GACCAGAAGAAGCCAGAAAATGGA-3', AI89LJ8_R 5'-TGTCCTGAGCAATAGCACTTTAAGAA-3', AI89LJ8_M FAM 5'-CCTCTGGTGCTAAAGTC-3'); Acvr1: custom designed TaqMan primer set to detect exon 7(AIKAL5S_F 5'-CTCACTACTCTGGATACGGTTAGCT-3', AIKAL5S_R 5'-GGGTCCCAAATATCTCTATGTGCAA-3', AIKAL5S_M FAM 5'-CTATGGACAGTACAATCCG-3')

Primary calvarial osteoblast isolation and culture

Calvarial pre-osteoblasts were isolated from the nasal-frontal bones of neonatal skulls as described previously (Mansukhani et al., 2000; Yu et al., 2005). Pre-osteoblasts were maintained in minimum essential medium (alpha-MEM) (Invitrogen, #12561) supplemented with 10% fetal bovine serum (Hyclone) and 1% of penicillin/streptomycin (Sigma, #P-0781). To prepare homozygous mutant pre-osteoblasts for Bmpr1a and Acvr1, isolated cells were treated with 100 ng/ml 4-hydroxytamoxifen for 6 days, exchanging media every other day before sorting. Cells were stained with fluorescein di β-D-galactopyranoside (FDG) and fractionated by FACS according to manufacturer's procedures for FluoReporter ® lacZ Flow Cytometry Kits (Thermo Fisher Scientific, #F-1930)(Komatsu et al., 2011). BMP2 treatment for pre-osteoblasts was done at 100ng/ml for 30 minutes (R&D, #355-BM).

Western blot analysis

Protein extracts were prepared either from frontal calvaria of postnatal day 3 mice or preosteoblasts isolated from calvaria as described above. Cells and tissues were lysed using RIPA buffer (20mM Tris-HCl, 0.1% SDS, 1% Triton X-100, 1% sodium deoxycholate). Subsequently, cell lysates were separated by 10% SDS-PAGE and transferred to PVDF membrane (Millipore, #IPVH00010). Immunoblotting was performed with a rabbit anti-phospho-Smad1/5/9 antibody (Cell signaling: #13820). Mouse anti-vinculin antibody (Sigma-Aldrich, #V4505) was used as a loading control. Signal detection was performed with ECL Western blotting detection reagents (GE Healthcare) and images were quantified by Image J software.

Gene silencing and Noggin treatment

siRNA for negative control (scrambled, #4390843), targeting Bmpr1a (#4390771, siRNAID s201097) and Acvr1 (#4390771, siRNAID s61924) were from Thermofisher. Sequences used in this study were as follows: sense siRNA for Bmpr1a, CAACAGUGAUACAAAUGAAtt; sense siRNA sequence for Acvr1, GAAUGGACAGUGCUGCAUAtt. Transfection procedure was performed according to Lipofectamine 2000 reagent (Invitrogen, #11668-027) protocol. Final siRNA amount was 25pmol for each 6-well dish. Three days after transfection, cells were treated with 100ng/ml Noggin (R &D systems, #6057-NG-CF) for 2 hours before collecting protein and RNA.

Results

Craniosynostosis phenotypes were partially rescued by a heterozygous null mutation of Bmpr1a, but not by those of Bmpr1b or Acvr1

Our previous studies indicated that enhanced BMP signaling through ca-BmpR1A in cranial neural crest cells leads to craniosynostosis (ca-Bmpr1a;P0-Cre or ca1A, hereafter), and that heterozygous null mutation of endogenous Bmpr1a can partially rescue the skull deformity (Komatsu et al., 2013). To evaluate if other BMP type I receptors are involved in transducing BMP signaling during the pathogenesis of craniosynostosis, we introduced individual BMP type I receptor null heterozygosity: ca- Bmpr1a;P0-Cre;Bmpr1a$^{+/-}$ (ca1A;1aH), ca-Bmpr1a;P0-Cre;Bmpr1b$^{+/-}$ (ca1A;1bH) and ca-Bmpr1a;P0-Cre;Acvr1$^{+/-}$ (ca1A;AcH). Unlike ca1A;1aH, the skull deformities were not rescued in either ca1A;1bH or ca1A;AcH mice (Fig. 1Ac-Ae). Both ca1A;1bH and ca1A;AcH still showed short snouts, wider distance between eyes and dome-shaped skull vaults similar to ca1A, while ca1A;1aH showed a largely normal nose and slightly dome head (Fig. 1A). Whole mount skeletal staining at postnatal day 17 (P17) demonstrated patent anterior frontal sutures in control (Cont, hereafter) and ca1A;1aH mice; there is no patent anterior frontal suture observed in ca1A, ca1A;1bH and ca1A;AcH mice (Fig. 1Af-Aj). We also observed large cavities in nasal and frontal bones in ca1A, ca1A;1bH and ca1A;AcH mice (Fig. 1Ag, Aj, Ak, An, Ao). Micro-CT analysis of frontal bones revealed a significant decrease (63% ($p<10^{-7}$), 66% ($p<10^{-6}$), and 75% ($p<10^{-8}$) respectively) in trabecular bone volume (BV/TV) in ca1A, ca1A;1bH and ca1A;AcH mice. In contrast, a lesser decrease in BV/TV (38%, $p<0.01$) was observed in ca1A;1aH mice (Fig. 1B). The average length from the nose tip to middle of the coronal suture was significantly decreased to 74%, 71% and 66% of control in mutant mice, ca1A;1bH mice and ca1A;AcH mice respectively. ca1A;1aH mice showed a milder decrease to 90% of control (Fig. 1C). Bmpr1b$^{-/-}$; ca-Bmpr1a;P0-Cre mice showed the same limb abnormalities same as in Bmpr1b$^{-/-}$ mice and the same skull deformities as caBmpr1a(+);P0Cre(+) mice (Komatsu et al., 2013; Yi et al., 2000) (Supplementary Fig. 1). Bmpr1b$^{-/-}$ mice without caA1 mutation did not develop any overt suture phenotypes (Supplementary Fig. 2). These results suggest that phenotypes developed in the ca-Bmpr1a;P0-Cre mice can only be rescued by Bmpr1a heterozygosity but not by Bmpr1b or Acvr1 heterozygosity.

To confirm the results from gross observations, we made histological assessments on all types of mutant and control mice at different stages. At birth (postnatal day 0), the stage

before any sign of clear premature fusion of the anterior frontal (AF) suture, we were able to observe decreased bone formation in ca1A mice (Fig. 2B, G). Additionally, von Kossa staining confirmed decreased mineral deposition, and abnormal calcification in the suture region. In contrast, ca1A;1aH showed no signs of abnormal calcification in the suture region in both histology and von Kossa staining similar to controls (Cont) (Fig. 2A, C, F, H). In ca1A;1bH and ca1A;AcH mice, we did not observe additional calcification in the suture region. Rather, we observed thicker staining domains at deeper positions in the frontal bones (Fig. 2D, E, I, J). At P9, bone ossification appeared to be irregular at the anterior frontal suture region (Fig. 2K–T). At this stage, the anterior frontal (AF) suture was prematurely fused in ca1A;1bH and ca1A;AcH mice (Fig. 2N, O), similar to that observed in ca1A (Fig. 2L). In contract, we observed patent the AF sutures in ca1A;1aH mice at P9, similar to Cont mice (Fig. 2M, K). Calvaria of ca1A, ca1A;1bH and ca1A;AcH mice were thinner, but the calvaria from ca1A;1aH mice showed similar thickness with those from Cont mice. On the other hand, in ca1A, ca1A;1aH, ca1A;1bH and ca1A;AcH mice, the coronal, sagittal, and lambdoidal sutures developed normally and are patent at newborns and P9 (data not shown). These histological assessments confirm that only heterozygous null mutation of Bmrp1a partially rescues the craniosynostosis caused by ca1A.

To investigate alterations in cellular phenotypes in each genotype, we measured presence of phospho-Smad1, 5, 9 (pSmad1/5/9) as a readout of BMP-Smad signaling, levels of apoptosis with TUNEL assay and cell proliferation with anti-Ki67 immunohistochemistry staining at E18.5. Calvaria of ca1A mice showed a robust increase of pSmad1/5/9 immunosignals and a narrow space between pSmad1/5/9 positive domains in the presentative anterior frontal suture (Fig. 3A, white bracket). Calvaria from ca1A;1aH mice showed more intensive pSmad1/5/9 signals, however, the space between pSmad1/5/9 positive domains was wider than that of caA1 mice. In contrast, calvaria from caA1;1bH and ca1A;AcH mice showed similar patterns of immunosignals with that of caA1 (Fig. 3A).

Proportions of TUNEL-positive cells in the mesenchyme of the midline and the calvaria in the all 4 genotypes were higher than those in control (Fig. 3A, B, n=3 or more). However, those in ca1A;1aH were significantly lower than those in caA1 mice. Proportions of TUNEL-positive cells in ca1A;1bH and ca1A;AcH were lower than ca1A, but higher than those in ca1A;1aH (Fig 3A, B). Levels of Ki67 positive cells in the same region did not show significant difference among the five groups (n=3, $p > 0.05$ for all combinations) (Fig. 3A, C).

We also examined the status of osteogenic differentiation in calvaria from each genotype using an antibody for Podoplanin, a marker for early osteocytes (Stern et al., 2012). We also visualized collagen fibers by picrosirius red staining (Kaku et al., 2016). No overt changes were found in both E18.5 and P9 samples (Supplementary Fig. 3 and Supplementary Fig. 4, respectively).

Bmpr1a, Bmpr1b and Acvr1 are differentially expressed during skull development. BmpR1A, BmpR1B and AcvR1 are structurally similar type I receptors, but their heterozygosity led to different efficacy in the rescue of skull deformities caused by enhanced BMP-Smad signaling. To examine the underline reasons, we performed a thorough analysis

on the level of expression levels of these receptors. We first examined the expression in nasal-frontal bones in Cont, ca1A, ca1A;1aH, ca1A;1bH and ca1A;AcH mice by quantitative reverse-transcribed PCR (qRT-PCR) at P3 (Fig. 4A). Comparisons of the relative expression levels of Bmpr1a, Acvr1, and Bmpr1b showed that Bmpr1b was expressed at extremely low levels (approx. 0.1% of Bmpr1a) in control and mice of the other four genotypes (Fig. 4). PCR results indicated that Bmpr1a mRNA levels decreased to 59% of that in Cont in ca1A;1aH, and Bmpr1b mRNA levels decreased to 67% of that in Cont in ca1A;1bH; while expression levels of Acvr1 were not affected in ca1A;AcH ($p>0.1$). Meanwhile, heterozygosity of Bmpr1a in ca1A;1aH, of Bmpr1b in ca1A;1bH and of Acvr1 in ca1A;AcH did not lead to changes in expression of other two BMP type I receptors (Fig. 4A,A'). Similarly, the expression levels of Bmpr1a and Bmpr1b in the corresponding heterozygote mutant skulls showed approximately 50% of reduction while expression of Acvr1 was not changed in $Acvr1^{+/-}$ mice (Fig. 4B, B'). Unlike the Bmpr1a null allele in which the promoter region is deleted, the Acvr1 null allele was made by deletion of exon 5 that is critical for its receptor kinase activity (Mishina et al., 1999; Mishina et al., 1995). Thus, all regions except exon 5 remain intact in the Acvr1 null allele that could explain comparable levels of Acvr1 expression in the heterozygous null tissues with those in controls.

Each type I receptor differentially contributes to BMP-Smad signaling

caBmpr1a; P0-Cre mutant mice showed increase levels of BMP signaling in neural crest-derived tissues including osteoblasts (Komatsu et al., 2013). To investigate the impact of heterozygous null mutations for each BMP type I receptor on BMP signaling in vivo, we examined the levels of phosphorylated Smad1/5/9 (pSmad1/5/9) in nasal and frontal bones. In ca1A;1aH mice, we observed apparent decrease of pSmad1/5/9 levels while in ca1A;1bH and ca1A;AcH mice, no obvious decreases was observed (Fig. 5A). Similarly, approximately 50% of reduction in BMP-Smad signaling was observed in nasal and frontal bones from $Bmpr1a^{+/-}$ mutant mice, whereas no alterations were observed in those of $Bmpr1b^{+/-}$ and $Acvr1^{+/-}$ mutant mice (Fig. 5B). Similarly, when in vitro induction of BMP signaling in pre-osteoblast suggested that loss of one copy or two copies of Bmpr1b showed no alterations in pSmad1/5/9, either (Supplementary Fig. 5). These results suggest the BmpR1A is the major type I receptor for transducing BMP signaling in preosteoblasts.

The lack of an impact of deletion of Bmpr1b on the mutant phenotypes can be explained by the very low expression of Bmpr1b in calvarial cells. However, Acvr1 is expressed in these cells but heterozygosity for this receptor does not rescue the mutant phenotypes. To determine the extent of involvement of AcvR1 to BMP-Smad signaling, we generated homozygous null pre-osteoblasts for Acvr1 to compare levels of pSmad1/5/9 with control and Bmpr1a mutant preosteoblasts. Since Bmpr1a and Acvr1 homozygous mutations lead to embryonic lethality at early gastrulation, we isolated pre-osteoblast from calvaria of Ubi-Cre^{ERT2};$Bmpr1a^{fx/-}$ and Ubi-Cre^{ERT2};$Acvr1^{fx/-}$ mice, and induced the deletion through in vitro treatment with tamoxifen. To further purify homozygous null cells, mice were also bred with ROSA26-LacZ Cre reporter line (Soriano, 1999) and tamoxifen-treated calvarial preosteoblasts that express beta-galactosidase were stained with a fluorescent substrate then enriched through cell sorting (Fig. 6A). For Bmpr1a, exon 4 is deleted in the null allele and

is floxed in the floxed allele (Mishina et al., 1999; Mishina et al., 2002). Both quantitative PCR on genomic DNA and qRT-PCR on Bmpr1a mRNA designed to detect exon 4 demonstrated a nearly complete deletion of Bmpr1a (Fig. 5B, left and right panels, respectively). Results shown in Fig. 4 suggest that the transcriptional activity of the Acvr1 null allele is comparable to that of the wild-type (wt) allele.

Genomic quantitative PCR detecting exon 7 of Acvr1 showed about 60% of reduction (expected value is 50% because Acvr1 null allele has intact exon 7), suggesting that Credependent recombination of exon 7 is nearly complete (Fig. 6C). The transcripts from the Cre-recombined Acvr1 allele (dE allele) lack exon 7 (Kaartinen and Nagy, 2001; Komatsu et al., 2007). Thus, efficiency of Acvr1 deletion was evaluated using RT-PCR amplifying between exon 4 and 8 by detecting a loss of either exon 5 or 7. After enrichment of LacZ expressing cells, we detected nearly no wt transcript for Acvr1 that contains both exon 5 and 7 (data not shown).

Subsequently, these pre-osteoblast cells were used to evaluate BMP signaling with BMP2 treatment (Fig. 6D). For the cells after FACS purification, only deletion of Bmpr1a led to significant decrease of pSmad1/5/9 levels, while deletion of Acvr1 led to nearly no impact on pSmad1/5/9 levels (Fig. 6D). These results confirmed our aforementioned finding that in calvarial pre-osteoblasts, BmpR1A, but not AcvR1 or BmpR1B transduces BMP-Smad signaling.

Previously mentioned data strongly suggest that endogenous BMPR1A has higher capacity to transduce BMP-Smad signaling than BMPR1B or ACVR1. However, it is possible that caBMPR1A transduce BMP-Smad signaling specifically through direct interaction with the endogenous BMPR1A, which would have nothing to do with endogenous BMPR1B or ACVR1. This is a plausible explanation because we previously show that a constitutively active form of BMP type 1 receptor requires presence of type 2 receptors (Bagarova et al., 2013). To exclude this possibility, we established primary preosteoblasts carrying caBmpr1a, but knocked-down expression of either Bmpr1a or Acvr1 by siRNA treatment. Levels of gene silencing were checked by Q-RT-PCR (Fig. 7, bottom). As expected, cells without Noggin treatment showed reduced pSmad1/5/9 levels when Bmpr1a was silenced suggesting that BMP ligands possibly from serum stimulates endogenous BMPR1A (Fig. 7, lane 1–3 and 7–9). Next, we treated the cells with Noggin to block ligands that could possibly be introduced into culture media through serum. In this condition, we expected most of the BMP-Smad signaling, if not all, induced by ligand-receptor interaction would be blocked, thus pSmad1/5/9 should reflect levels of BMP-SMAD signaling transduced by caBMPR1A. Western blot analyses to measure levels of pSmad1/5/9 demonstrated that BMP-Smad signaling levels are comparable between control and each receptor knocked-down cells in the caBmpr1a mutant cells with Noggin (Fig. 7, lane 10–12), and higher than those in control cells treated with Noggin (Fig. 7, lane 4–6). These results strongly suggest that caBMPR1A transduced BMP-Smad signaling does not require a specific BMP type 1 receptor.

Discussion

Our previous work indicated that enhanced BMP signaling in neural crest cells resulted in pre-mature fusion of anterior frontal sutures in mice (Komatsu et al., 2013). Here we demonstrated that the skull deformity phenotypes, including short nose, prematurely fused sutures and domed skull shape, which are observed in the mutant mice were largely rescued by heterozygous null mutation of endogenous Bmpr1a, but not by that of Bmpr1b or Acvr1, revealing different contributions of each receptor in skull development. Our mechanistic studies further suggest that in calvarial pre-osteoblasts, BmpR1A is the major type I receptor in transducing BMP-Smad signaling. Overall, our work presented here demonstrates the first effort to identify a specific BMP type I receptor for skull development and potential involvement of craniosynostosis.

BmpR1A, BmpR1B and AcvR1 are BMP type 1 receptors with highly similar structures. They can individually activate BMP signaling upon ligand binding (Chen et al., 2004; Koenig et al., 1994; Kotzsch et al., 2008). Each type 1 receptor shows different affinities to distinct BMP ligands (Graff et al., 1994; Koenig et al., 1994; Suzuki et al., 1994; ten Dijke et al., 1994). Different phenotypes found in their homozygous mutant mice demonstrated that BMP signaling mediated by each receptor has unique tissue functions (Mishina et al., 1999; Mishina et al., 1995; Rigueur et al., 2015; Yi et al., 2000; Yoon et al., 2005). The expression patterns and levels of Bmpr1a and Bmpr1b are different in chick and mouse (Merrill et al., 2008; Yoon et al., 2005). Similarly, different and restricted functions and expression levels of three type I receptors for BMPs were observed in this study. All of this prompted us to understand if the various BMP type I receptors play differential roles in skull development and in craniosynostosis.

BMP signaling is mediated by intracellular signal transducers Smads1/5/9. Premature fusion of cranial sutures in ca-Bmpr1a;P0-Cre mice was attributed to an increase in Smad signaling. Previous studies have demonstrated that Smads1, −4 and −5 are required for skeletogenesis (Retting et al., 2009; Tan et al., 2007). Osteoblast-specific Smad1 or Smad4 mutants showed decreased bone formation (Tan et al., 2007; Wang et al., 2011). As expected, heterozygous null mutation of Bmpr1b resulted in 50% reduction of Bmpr1b expression in ca1A;1bH and Bmpr1b$^{+/-}$ (Fig. 4A', B'). However, Phospho- Smad1/5/9 levels did not decrease accordingly in the nasal and frontal bones in ca1A;1bH or Bmpr1b$^{+/-}$ mice (Fig. 5). Our in vitro cellular mechanistic studies further indicated that haploinsufficiency or even the knockout of Bmpr1b did not apparently affect cellular response to BMP ligands (Shi et al., 2016). Consistent with this, we observed that homozygous knockout of Bmpr1b did not rescue skull deformities (Supplementary Fig. 1). Together with the observation that Bmpr1b is expressed at low levels in the skull, it is likely that BMP signaling mediated by BmpR1B does not play a significant role during skull development.

Our in vivo and in vitro studies also indicated that deletion of Acvr1 did not alter levels of BMP-Smad signaling either. These results suggested that the role of AcvR1 in transducing BMP-Smad signaling is limited to calvarial pre-osteoblasts. Indeed, very small changes in pSmad1/5/9 levels have been reported in conditional Acvr1 mutants (Dudas et al., 2004;

Rigueur et al., 2015). On the other hand, a number of studies showed dramatic decrease of pSmad1/5/9 level in Bmpr1a conditional knockout studies (Andl et al., 2004; Huang et al., 2014; Kamiya et al., 2008b; Murali et al., 2005), further suggesting the primary role of BmpR1A in BMP-Smad signaling in vivo as well.

Our previous studies demonstrated that osteoblast-specific Acvr1 mutants show nearly identical phenotypes to those found in an osteoblast-specific knockout of Bmpr1a (Kamiya et al., 2010; Kamiya and Mishina, 2011; Kamiya et al., 2008a; Kamiya et al., 2008b). Together with our current data, it is tempting to speculate that in the Acvr1 mutant osteoblasts still maintain normal levels of BMP-Smad signaling activity and thus the phenotypes are likely caused by a loss of non-Smad signaling activity such as a TAK1-mediated signaling pathway. Similarly, we previously reported that compound homozygous mutant embryos for Bmpr1a (cKO with Col2a1-Cre) and Bmpr1b develop severely reduced cartilage, whereas mutant embryos deficient either for Bmpr1a or Bmpr1b develop relatively normal cartilage primordia (Yoon et al., 2005). It is possible that BMP-Smad signaling levels in double mutant embryos are similar to those seen in Bmpr1a cKOs, but further alterations in non-Smad signaling by compound mutations of Bmpr1a and Bmpr1b results in severe phenotypes in chondrogenesis. Further studies are needed to address this possibility.

Overall, our in vivo and in vitro data in this study suggest that BmpR1A but not BmpR1B or AcvR1 is the key BMP type I receptor that transduces BMP-Smad signaling during calvarial bone development. BmpR1A is solely responsible for the pathogenetic changes found in the craniosynostosis mouse model caused by an increase of BMP-Smad signaling in neural crest cells. Although no human craniosynostosis case has been reported with mutations in BMPR1A, there are several pieces of supporting evidence to hypothesize that BMPR1A may play a pivotal role for pathogenesis of craniosynostosis. Recent genome-wide association studies (GWAS) identify several single-nucleotide polymorphisms (SNPs) associated with non-syndromic midline craniosynostosis. The most significant SNP is located close to BMP2 that prompted to hypothesize that this region may act as an enhancer for BMP2 (Justice et al., 2012) and resulted augmentation of BMP signaling is the molecular reason of the pathogenesis (a BMP2 risk allele). A recent publication demonstrates that in non-syndromic midline craniosynostosis only 9% penetrance for SMAD6 mutations and 0.08 % for the BMP2 risk allele, but 100% penetrance is observed when both alleles are present in one individual (Komatsu and Mishina, 2016; Timberlake et al., 2016). Since SMAD6 negatively regulates BMP-Smad signaling, it is reasonable to speculate that increased BMP-Smad signaling due to the bigenic mutations in BMP2 and SMD6 genes is a cause of premature suture fusion in these patients (Komatsu and Mishina, 2016; Timberlake et al., 2016). Based on our findings described in this submission, it is tempting to speculate that BMPR1A is the type 1 receptor responsible for the pathogenesis of these clinical cases.

Supplementary Material

Refer to Web version on PubMed Central for supplementary material.

Acknowledgments

We gratefully acknowledge Dr. Michelle Lynch for technical support of microCT images, Drs. Satoru Hayano and Ce Shi for advices on research strategy, Drs. Manas Ray and Kaitrin Kramer for critical reading of this manuscript. We thank Mr. Anshul Kulkarni, Ms. Folasade Adegbenro, and Ms. Kristen Kelly for helping analyses of microCT images. We also thank Dr. Kenichi Yamamura for providing P0-Cre mice. This study is supported by the National Institutes of Health (R00DE021054 to Y.K., R01DE013085 to V.K., R01DE020843 to Y.M., and S10RR026475-01 to the School of Dentistry microCT Core).

Authors' roles: Study design: HP, YK and YM. Study conduct, data collection, and data analysis: HP, HZ, PA and YM. Provide critical materials: YK, KL, VK and YM: Drafting manuscript: HP and YM. Approving final version of manuscript: HP, HZ, PA, YK, KL, VK, and YM. HP and YM take responsibility for the integrity of the data analysis.

References

Andl T, Ahn K, Kairo A, Chu EY, Wine-Lee L, Reddy ST, Croft NJ, Cebra- Thomas JA, Metzger D, Chambon P, Lyons KM, Mishina Y, Seykora JT, Crenshaw EB 3rd, Millar SE. Epithelial Bmpr1a regulates differentiation and proliferation in postnatal hair follicles and is essential for tooth development. Development. 2004; 131:2257–2268. DOI: 10.1242/dev.01125 [PubMed: 15102710]

Bagarova J, Vonner AJ, Armstrong KA, Borgermann J, Lai CS, Deng DY, Beppu H, Alfano I, Filippakopoulos P, Morrell NW, Bullock AN, Knaus P, Mishina Y, Yu PB. Constitutively active ALK2 receptor mutants require type II receptor cooperation. Mol Cell Biol. 2013; 33:2413–2424. DOI: 10.1128/MCB.01595-12 [PubMed: 23572558]

Baur ST, Mai JJ, Dymecki SM. Combinatorial signaling through BMP receptor IB and GDF5: shaping of the distal mouse limb and the genetics of distal limb diversity. Development. 2000; 127:605–619. [PubMed: 10631181]

Chen D, Zhao M, Mundy GR. Bone morphogenetic proteins. Growth Factors. 2004; 22:233–241. DOI: 10.1080/08977190412331279890 [PubMed: 15621726]

de Caestecker M. The transforming growth factor-beta superfamily of receptors. Cytokine Growth Factor Rev. 2004; 15:1–11. [PubMed: 14746809]

Dudas M, Sridurongrit S, Nagy A, Okazaki K, Kaartinen V. Craniofacial defects in mice lacking BMP type I receptor Alk2 in neural crest cells. Mech Dev. 2004; 121:173–182. DOI: 10.1016/j.mod.2003.12.003 [PubMed: 15037318]

Graff JM, Thies RS, Song JJ, Celeste AJ, Melton DA. Studies with a Xenopus BMP receptor suggest that ventral mesoderm-inducing signals override dorsal signals in vivo. Cell. 1994; 79:169–179. [PubMed: 7522972]

Gu Z, Reynolds EM, Song J, Lei H, Feijen A, Yu L, He W, MacLaughlin DT, van den Eijnden-van Raaij J, Donahoe PK, Li E. The type I serine/threonine kinase receptor ActRIA (ALK2) is required for gastrulation of the mouse embryo. Development. 1999; 126:2551–2561. [PubMed: 10226013]

Hayano S, Komatsu Y, Pan H, Mishina Y. Augmented BMP signaling in the neural crest inhibits nasal cartilage morphogenesis by inducing p53-mediated apoptosis. Development. 2015; 142:1357–1367. DOI: 10.1242/dev.118802 [PubMed: 25742798]

Heldin CH, Miyazono K, ten Dijke P. TGF-beta signalling from cell membrane to nucleus through SMAD proteins. Nature. 1997; 390:465–471. DOI: 10.1038/37284 [PubMed: 9393997]

Hogan, B. Manipulating the mouse embryo : a laboratory manual. 2. Cold Spring Harbor Laboratory Press; Plainview, N.Y.: 1994.

Huang P, Schulz TJ, Beauvais A, Tseng YH, Gussoni E. Intramuscular adipogenesis is inhibited by myo-endothelial progenitors with functioning Bmpr1a signalling. Nat Commun. 2014; 5:4063.doi: 10.1038/ncomms5063 [PubMed: 24898859]

Ishii M, Han J, Yen HY, Sucov HM, Chai Y, Maxson RE Jr. Combined deficiencies of Msx1 and Msx2 cause impaired patterning and survival of the cranial neural crest. Development. 2005; 132:4937–4950. DOI: 10.1242/dev.02072 [PubMed: 16221730]

Justice CM, Yagnik G, Kim Y, Peter I, Jabs EW, Erazo M, Ye X, Ainehsazan E, Shi L, Cunningham ML, Kimonis V, Roscioli T, Wall SA, Wilkie AO, Stoler J, Richtsmeier JT, Heuze Y, Sanchez-Lara PA, Buckley MF, Druschel CM, Mills JL, Caggana M, Romitti PA, Kay DM, Senders C, Taub PJ,

Klein OD, Boggan J, Zwienenberg-Lee M, Naydenov C, Kim J, Wilson AF, Boyadjiev SA. A genome-wide association study identifies susceptibility loci for nonsyndromic sagittal craniosynostosis near BMP2 and within BBS9. Nat Genet. 2012; 44:1360–1364. ng.2463 [pii]. DOI: 10.1038/ng.2463 [PubMed: 23160099]

Kaartinen V, Dudas M, Nagy A, Sridurongrit S, Lu MM, Epstein JA. Cardiac outflow tract defects in mice lacking ALK2 in neural crest cells. Development. 2004; 131:3481–3490. DOI: 10.1242/dev.01214 [PubMed: 15226263]

Kaartinen V, Nagy A. Removal of the floxed neo gene from a conditional knockout allele by the adenoviral Cre recombinase in vivo. Genesis. 2001; 31:126–129. [PubMed: 11747203]

Kaku M, Rosales Rocabado JM, Kitami M, Ida T, Akiba Y, Yamauchi M, Uoshima K. Mechanical Loading Stimulates Expression of Collagen Cross-Linking Associated Enzymes in Periodontal Ligament. J Cell Physiol. 2016; 231:926–933. DOI: 10.1002/jcp.25184 [PubMed: 26381152]

Kamiya N, Kobayashi T, Mochida Y, Yu PB, Yamauchi M, Kronenberg HM, Mishina Y. Wnt inhibitors Dkk1 and Sost are downstream targets of BMP signaling through the type IA receptor (BMPRIA) in osteoblasts. J Bone Miner Res. 2010; 25:200–210. DOI: 10.1359/jbmr.090806 [PubMed: 19874086]

Kamiya N, Mishina Y. New insights on the roles of BMP signaling in bone-A review of recent mouse genetic studies. Biofactors. 2011; 37:75–82. DOI: 10.1002/biof.139 [PubMed: 21488130]

Kamiya N, Ye L, Kobayashi T, Lucas DJ, Mochida Y, Yamauchi M, Kronenberg HM, Feng JQ, Mishina Y. Disruption of BMP signaling in osteoblasts through type IA receptor (BMPRIA) increases bone mass. J Bone Miner Res. 2008a; 23:2007–2017. DOI: 10.1359/jbmr.080809 [PubMed: 18684091]

Kamiya N, Ye L, Kobayashi T, Mochida Y, Yamauchi M, Kronenberg HM, Feng JQ, Mishina Y. BMP signaling negatively regulates bone mass through sclerostin by inhibiting the canonical Wnt pathway. Development. 2008b; 135:3801–3811. dev.025825 [pii]. DOI: 10.1242/dev.025825 [PubMed: 18927151]

Kim HJ, Rice DP, Kettunen PJ, Thesleff I. FGF-, BMP- and Shh-mediated signalling pathways in the regulation of cranial suture morphogenesis and calvarial bone development. Development. 1998; 125:1241–1251. [PubMed: 9477322]

Koenig BB, Cook JS, Wolsing DH, Ting J, Tiesman JP, Correa PE, Olson CA, Pecquet AL, Ventura F, Grant RA, et al. Characterization and cloning of a receptor for BMP-2 and BMP-4 from NIH 3T3 cells. Mol Cell Biol. 1994; 14:5961–5974. [PubMed: 8065329]

Komatsu Y, Kaartinen V, Mishina Y. Cell cycle arrest in node cells governs ciliogenesis at the node to break left-right symmetry. Development. 2011; 138:3915–3920. dev.068833 [pii]. DOI: 10.1242/dev.068833 [PubMed: 21831921]

Komatsu Y, Mishina Y. An epistatic explanation. Elife. 2016; 5doi: 10.7554/eLife.21162

Komatsu Y, Scott G, Nagy A, Kaartinen V, Mishina Y. BMP type I receptor ALK2 is essential for proper patterning at late gastrulation during mouse embryogenesis. Dev Dyn. 2007; 236:512–517. DOI: 10.1002/dvdy.21021 [PubMed: 17117439]

Komatsu Y, Yu PB, Kamiya N, Pan H, Fukuda T, Scott GJ, Ray MK, Yamamura K, Mishina Y. Augmentation of Smad-dependent BMP signaling in neural crest cells causes craniosynostosis in mice. J Bone Miner Res. 2013; 28:1422–1433. DOI: 10.1002/jbmr.1857 [PubMed: 23281127]

Kotzsch A, Nickel J, Seher A, Heinecke K, van Geersdaele L, Herrmann T, Sebald W, Mueller TD. Structure analysis of bone morphogenetic protein-2 type I receptor complexes reveals a mechanism of receptor inactivation in juvenile polyposis syndrome. J Biol Chem. 2008; 283:5876–5887. DOI: 10.1074/jbc.M706029200 [PubMed: 18160401]

Lajeunie E, Le Merrer M, Bonaiti-Pellie C, Marchac D, Renier D. Genetic study of nonsyndromic coronal craniosynostosis. Am J Med Genet. 1995; 55:500–504. DOI: 10.1002/ajmg.1320550422 [PubMed: 7762595]

Liu B, Yu HM, Hsu W. Craniosynostosis caused by Axin2 deficiency is mediated through distinct functions of beta-catenin in proliferation and differentiation. Dev Biol. 2007; 301:298–308. S0012-1606(06)01312-1 [pii]. DOI: 10.1016/j.ydbio.2006.10.018 [PubMed: 17113065]

Livak KJ, Schmittgen TD. Analysis of relative gene expression data using realtime quantitative PCR and the 2(−Delta Delta C(T)) Method. Methods. 2001; 25:402–408. DOI: 10.1006/meth.2001.1262 [PubMed: 11846609]

Mansukhani A, Bellosta P, Sahni M, Basilico C. Signaling by fibroblast growth factors (FGF) and fibroblast growth factor receptor 2 (FGFR2)-activating mutations blocks mineralization and induces apoptosis in osteoblasts. J Cell Biol. 2000; 149:1297–1308. [PubMed: 10851026]

Merrill AE, Eames BF, Weston SJ, Heath T, Schneider RA. Mesenchyme- dependent BMP signaling directs the timing of mandibular osteogenesis. Development. 2008; 135:1223–1234. DOI: 10.1242/dev.015933 [PubMed: 18287200]

Mishina Y, Crombie R, Bradley A, Behringer RR. Multiple roles for activin- like kinase-2 signaling during mouse embryogenesis. Dev Biol. 1999; 213:314–326. DOI: 10.1006/dbio.1999.9378 [PubMed: 10479450]

Mishina Y, Hanks MC, Miura S, Tallquist MD, Behringer RR. Generation of Bmpr/Alk3 conditional knockout mice. Genesis. 2002; 32:69–72. [PubMed: 11857780]

Mishina Y, Snider TN. Neural crest cell signaling pathways critical to cranial bone development and pathology. Exp Cell Res. 2014; S00144827(14)00037-8 [pii]. doi: 10.1016/j.yexcr.2014.01.019

Mishina Y, Suzuki A, Ueno N, Behringer RR. Bmpr encodes a type I bone morphogenetic protein receptor that is essential for gastrulation during mouse embryogenesis. Genes Dev. 1995; 9:3027–3037. [PubMed: 8543149]

Morriss-Kay GM, Wilkie AO. Growth of the normal skull vault and its alteration in craniosynostosis: insights from human genetics and experimental studies. J Anat. 2005; 207:637–653. DOI: 10.1111/j.1469-7580.2005.00475.x [PubMed: 16313397]

Murali D, Yoshikawa S, Corrigan RR, Plas DJ, Crair MC, Oliver G, Lyons KM, Mishina Y, Furuta Y. Distinct developmental programs require different levels of Bmp signaling during mouse retinal development. Development. 2005; 132:913–923. DOI: 10.1242/dev.01673 [PubMed: 15673568]

Retting KN, Song B, Yoon BS, Lyons KM. BMP canonical Smad signaling through Smad1 and Smad5 is required for endochondral bone formation. Development. 2009; 136:1093–1104. DOI: 10.1242/dev.029926 [PubMed: 19224984]

Rigueur D, Brugger S, Anbarchian T, Kim JK, Lee Y, Lyons KM. The type I BMP receptor ACVR1/ALK2 is required for chondrogenesis during development. J Bone Miner Res. 2015:733–741. [PubMed: 25413979]

Shi C, Iura A, Terajima M, Liu F, Lyons K, Pan H, Zhang H, Yamauchi M, Mishina Y, Sun H. Deletion of BMP receptor type IB decreased bone mass in association with compromised osteoblastic differentiation of bone marrow mesenchymal progenitors. Sci Rep. 2016; 6:24256.doi: 10.1038/srep24256 [PubMed: 27048979]

Snider TN, Mishina Y. Cranial neural crest cell contribution to craniofacial formation, pathology, and future directions in tissue engineering. Birth Defects Res C Embryo Today. 2014; 102:324–332. DOI: 10.1002/bdrc.21075 [PubMed: 25227212]

Soriano P. Generalized lacZ expression with the ROSA26 Cre reporter strain. Nat Genet. 1999; 21:70–71. DOI: 10.1038/5007 [PubMed: 9916792]

Stern AR, Stern MM, Van Dyke ME, Jahn K, Prideaux M, Bonewald LF. Isolation and culture of primary osteocytes from the long bones of skeletally mature and aged mice. Biotechniques. 2012; 52:361–373. DOI: 10.2144/0000113876 [PubMed: 22668415]

Suzuki A, Thies RS, Yamaji N, Song JJ, Wozney JM, Murakami K, Ueno N. A truncated bone morphogenetic protein receptor affects dorsal-ventral patterning in the early Xenopus embryo. Proc Natl Acad Sci U S A. 1994; 91:10255–10259. [PubMed: 7937936]

Tan X, Weng T, Zhang J, Wang J, Li W, Wan H, Lan Y, Cheng X, Hou N, Liu H, Ding J, Lin F, Yang R, Gao X, Chen D, Yang X. Smad4 is required for maintaining normal murine postnatal bone homeostasis. J Cell Sci. 2007; 120:2162–2170. DOI: 10.1242/jcs.03466 [PubMed: 17550966]

ten Dijke P, Yamashita H, Ichijo H, Franzen P, Laiho M, Miyazono K, Heldin CH. Characterization of type I receptors for transforming growth factorbeta and activin. Science. 1994; 264:101–104. [PubMed: 8140412]

Timberlake AT, Choi J, Zaidi S, Lu Q, Nelson-Williams C, Brooks ED, Bilguvar K, Tikhonova I, Mane S, Yang JF, Sawh-Martinez R, Persing S, Zellner EG, Loring E, Chuang C, Galm A, Hashim PW,

Steinbacher DM, DiLuna ML, Duncan CC, Pelphrey KA, Zhao H, Persing JA, Lifton RP. Two locus inheritance of non-syndromic midline craniosynostosis via rare SMAD6 and common BMP2 alleles. Elife. 2016; 5doi: 10.7554/eLife.20125

Twigg SR, Wilkie AO. A Genetic-Pathophysiological Framework for Craniosynostosis. Am J Hum Genet. 2015; 97:359–377. DOI: 10.1016/j.ajhg.2015.07.006 [PubMed: 26340332]

Urist MR. Bone: formation by autoinduction. Science. 1965; 150:893–899. [PubMed: 5319761]

Wang M, Jin H, Tang D, Huang S, Zuscik MJ, Chen D. Smad1 plays an essential role in bone development and postnatal bone formation. Osteoarthritis Cartilage. 2011; 19:751–762. DOI: 10.1016/j.joca.2011.03.004 [PubMed: 21420501]

Wilkie AO, Byren JC, Hurst JA, Jayamohan J, Johnson D, Knight SJ, Lester T, Richards PG, Twigg SR, Wall SA. Prevalence and complications of single-gene and chromosomal disorders in craniosynostosis. Pediatrics. 2010; 126:e391–400. DOI: 10.1542/peds.2009-3491 [PubMed: 20643727]

Wilkie AO, Morriss-Kay GM. Genetics of craniofacial development and malformation. Nat Rev Genet. 2001; 2:458–468. DOI: 10.1038/35076601 [PubMed: 11389462]

Yamauchi Y, Abe K, Mantani A, Hitoshi Y, Suzuki M, Osuzu F, Kuratani S, Yamamura K. A novel transgenic technique that allows specific marking of the neural crest cell lineage in mice. Dev Biol. 1999; 212:191–203. S0012160699993235 [pii]. DOI: 10.1006/dbio.1999.9323 [PubMed: 10419695]

Yi SE, Daluiski A, Pederson R, Rosen V, Lyons KM. The type I BMP receptor BMPRIB is required for chondrogenesis in the mouse limb. Development. 2000; 127:621–630. [PubMed: 10631182]

Yoon BS, Ovchinnikov DA, Yoshii I, Mishina Y, Behringer RR, Lyons KM. Bmpr1a and Bmpr1b have overlapping functions and are essential for chondrogenesis in vivo. Proc Natl Acad Sci U S A. 2005; 102:5062–5067. DOI: 10.1073/pnas.0500031102 [PubMed: 15781876]

Yoon BS, Pogue R, Ovchinnikov DA, Yoshii I, Mishina Y, Behringer RR, Lyons KM. BMPs regulate multiple aspects of growth-plate chondrogenesis through opposing actions on FGF pathways. Development. 2006; 133:4667–4678. DOI: 10.1242/dev.02680 [PubMed: 17065231]

Yu HM, Jerchow B, Sheu TJ, Liu B, Costantini F, Puzas JE, Birchmeier W, Hsu W. The role of Axin2 in calvarial morphogenesis and craniosynostosis. Development. 2005; 132:1995–2005. 132/8/1995 [pii]. DOI: 10.1242/dev.01786 [PubMed: 15790973]

Highlights

- BMPR1A is a major type 1 receptor for BMP-Smad signaling in the craniofacial region.
- Heterozygosity of Bmpr1a partially rescues craniosynostosis in caBmpr1a;P0Cre mice.
- Heterozygosity of other BMP type 1 receptor does not rescue craniosynostosis in mice.
- Each BMP type 1 receptor differentially contribute BMP-Smad signaling.
- These results suggest differential involvement of each receptor in craniosynostoses.

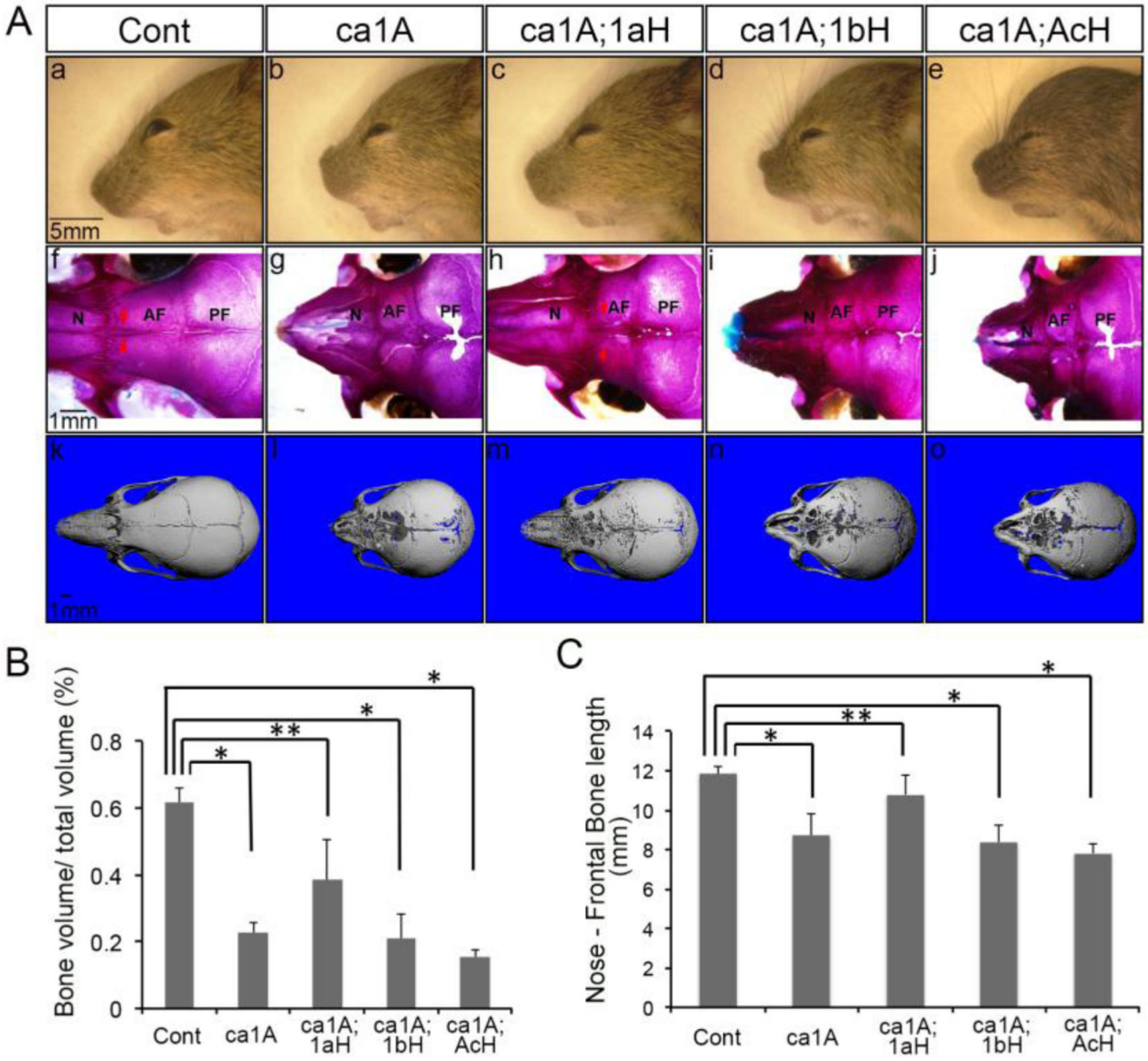

Fig. 1.

Skull deformities developed in caBmpr1a;P0-Cre mice were rescued by a heterozygosity of Bmpr1a. (A) (a–e) ca-Bmpr1a;P0-Cre;Bmpr1b$^{+/-}$ (ca1A;1bH) and ca-Bmpr1a;P0-Cre;Acvr1$^{+/-}$ (ca1A;AcH) displayed short, broad snouts and hypertelorism same as ca-Bmpr1a;P0-Cre (ca1A) while ca-Bmpr1a;P0-Cre;Bmpr1a$^{+/-}$ (ca1A;1aH) showed phenotypes similar to Control (Cont) at P17. (f–j) Skeletal staining at P17 revealed premature fusion at the anterior frontal (AF) suture in ca1A, ca1A;1bH and ca1A;AcH whereas the AF suture in Cont and ca1A;1aH was still patent. (k–o) MicroCT image showed more skull cavities in ca1A, ca1A;1bH and ca1A;AcH compared with ca1A;1aH. (B) Bone volume (BV/TV) in nasal and frontal bones were quantified by microCT. Data presented were means ± SD of five different skulls and three independent experiments. AF, anterior

frontal suture; N, nasal bone; PF, posterior frontal suture. n=5 per group, * $p<1\times10^{-6}$, ** $p<0.01$.

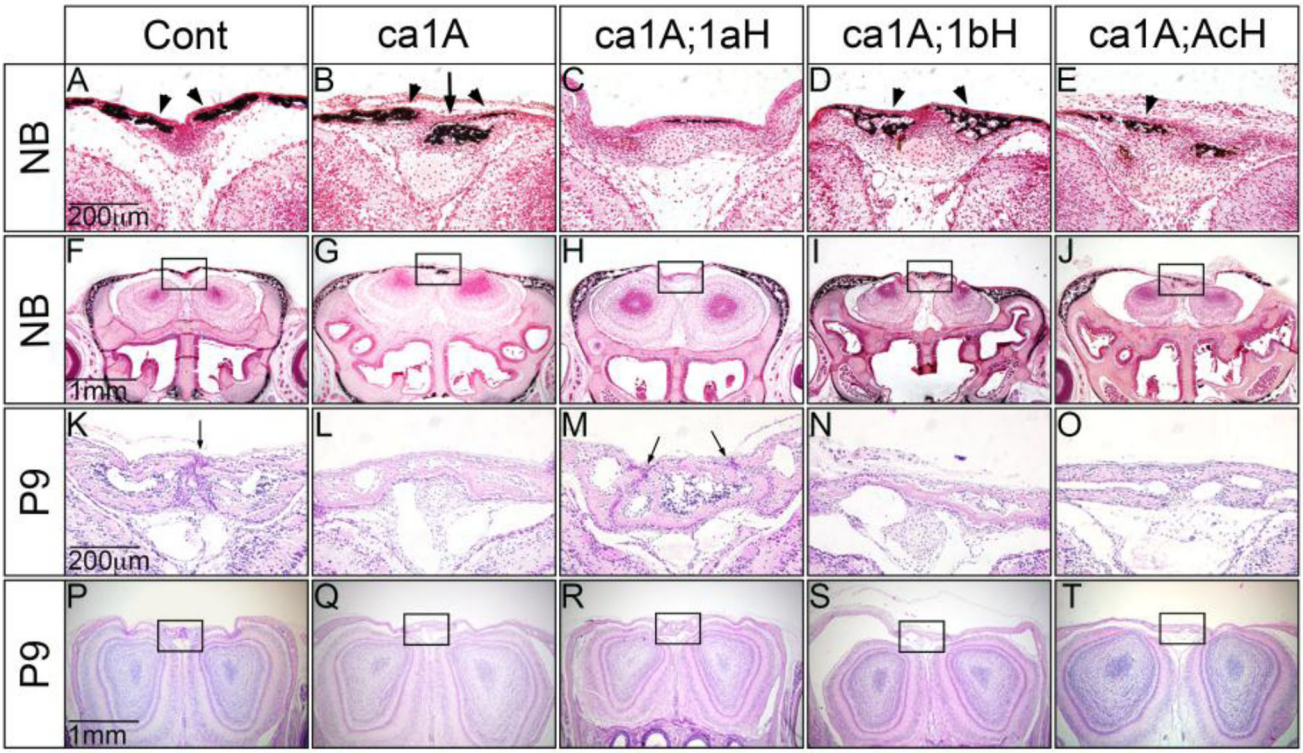

Fig. 2.

Histologic observation of sutures and mineral deposition in the anterior frontal bone of Cont, ca1A, ca1A;1aH, ca1A;1bH and ca1A;AcH mice. (A–J) Mineral deposition visualized by Von Kossa staining demonstrated that abnormal mineralized domains in the anterior frontal (AF) suture of ca1A, ca1A;1bH and ca1A;AcH mice at newborn. (K–T) Histological sections at P9 showed that the frontal sutures were prematurely fused in the ca1A, ca1A;1bH and ca1A;AcH mice; but were kept patent in Cont and ca1A;1aH mice. Scale bars: 100 μm in A and B; 200 μm in C–G; 50 μm in H and I.

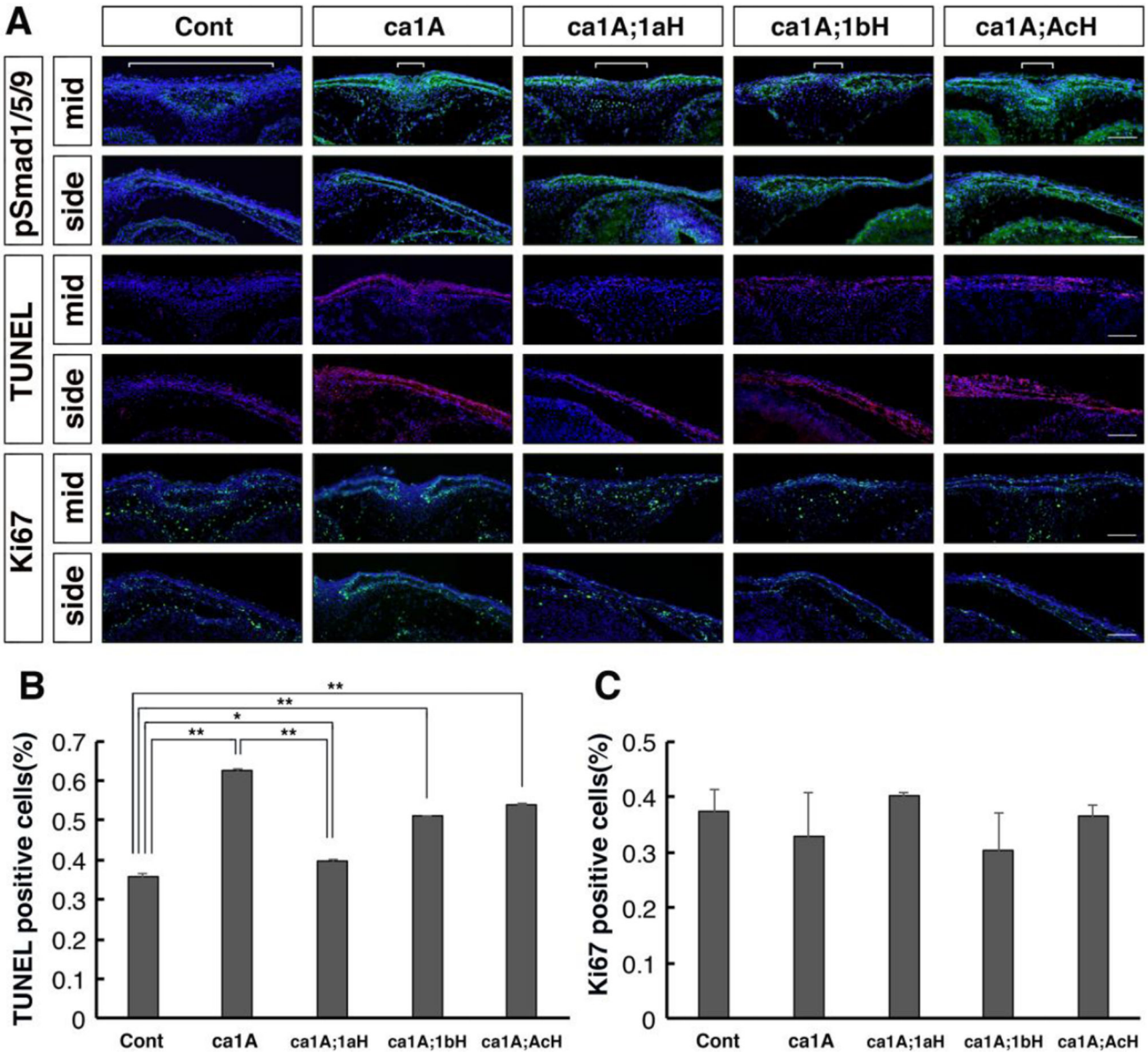

Fig. 3.

Levels of BMP-Smad signaling, cell death and proliferation were examined by immunohistochemistry. (A) Frontal sections (eye levels) of E18.5 calvaria from five genotypes of mice that include the presumptive anterior frontal sutures were used for immunodetection of pSmad1/5/9 (green), cell death (TUNEL assay, red)) and Ki67 (green), respectively. White brackets indicate a space between pSmad1/5/9 positive domains. (B, C) Quantification of TUNEL positive and Ki67 positive cells, respectively (n=3). *, $p<0.05$, **, $p<0.001$. Scale bars: 100 μm.

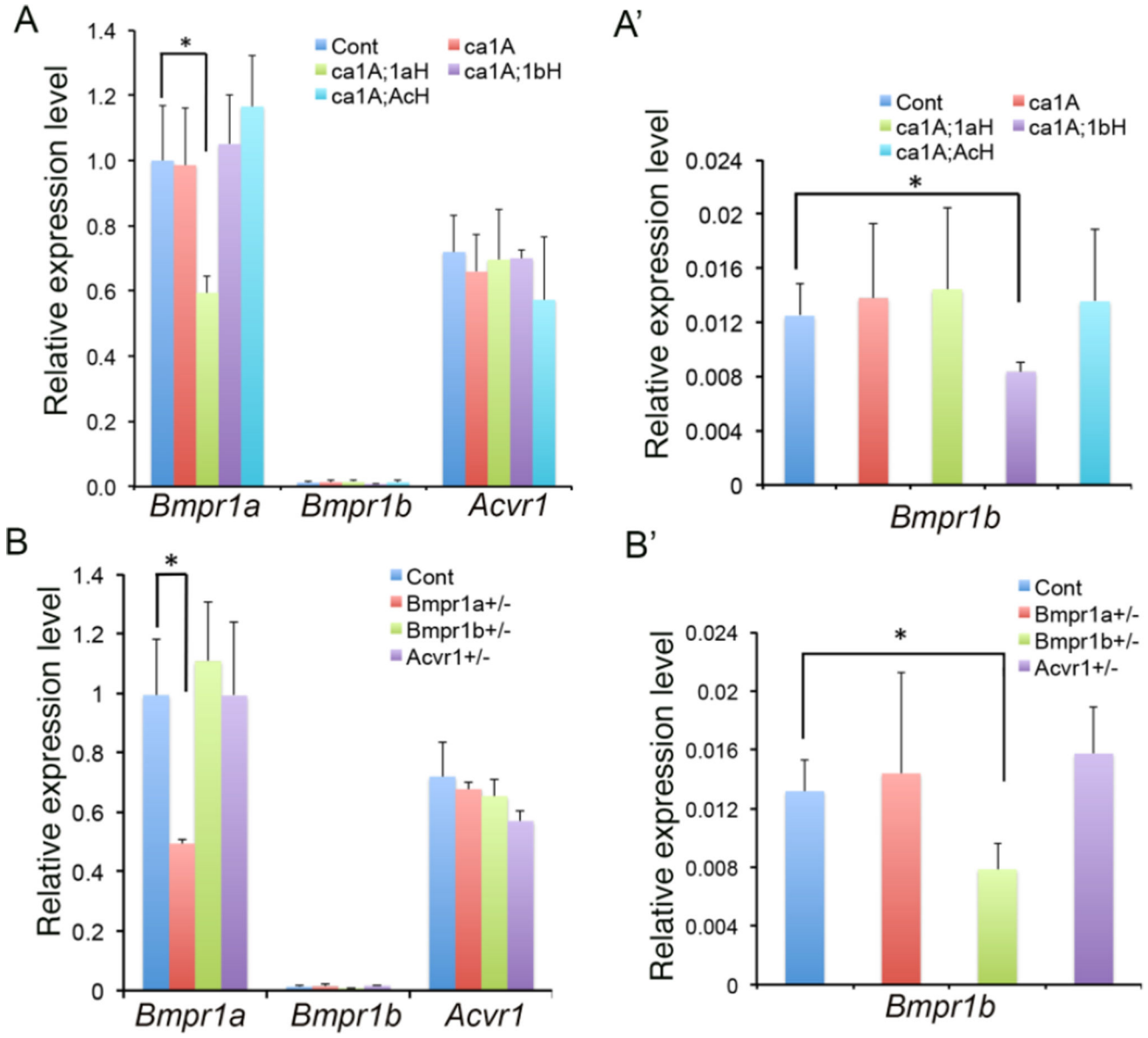

Fig. 4.

Expressions of Bmpr1a, Bmpr1b and Acvr1 were examined by quantitative real-time PCR (qRT-PCR). (A) Expression levels of Bmpr1a, Bmpr1b and Acvr1 were measured from nasal-frontal bone tissues of indicated genotypes of mice at P3. (A') Expression levels of Bmpr1b were examined from nasal-frontal bone tissues of indicated genotypes of mice at P3. (Enlarged expression levels of Bmpr1b part in A.) (B) Expressions of Bmpr1a, Bmpr1b and Acvr1 were examined from the nasal and the frontal bones of Cont, $Bmpr1a^{+/-}$, $Bmpr1b^{+/-}$ and $Acvr1^{+/-}$ mice at P3. (B') Expressions of Bmpr1b were examined from the nasal and the frontal bones of Cont, $Bmpr1a^{+/-}$, $Bmpr1b^{+/-}$ and $Acvr1^{+/-}$ mice at P3. (Enlarged expression levels of Bmpr1b part in B.) n>4 per group. * $p<0.05$.

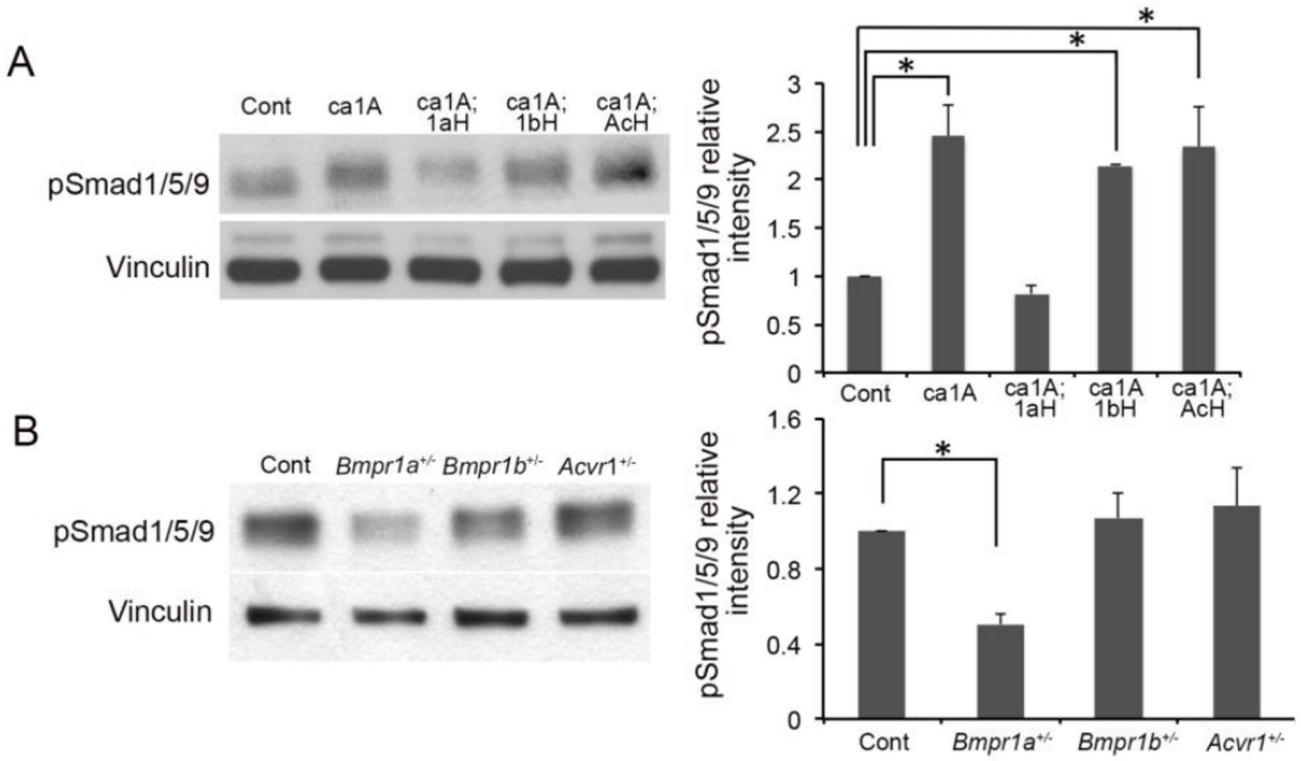

Fig. 5.

Enhanced BMP signaling is responsible for development of craniosynostosis. (A) Levels of Phospho-Smad1/5/9 (pSmad1/5/9) were examined by Western blotting using protein samples extracted from nasal-frontal bone of Cont, ca1A, ca1A;1aH, ca1A;1bH and ca1A;AcH mice at P3. (B) Levels of Phospho-Smad1/5/9 were examined using protein samples extracted from nasal-frontal bone of Cont, Bmpr1a$^{+/-}$, Bmpr1b$^{+/-}$ and Acvr1^{+-} mice at P3. Western blot results were quantified by densitometry (Image J). n=3, * $p<0.05$.

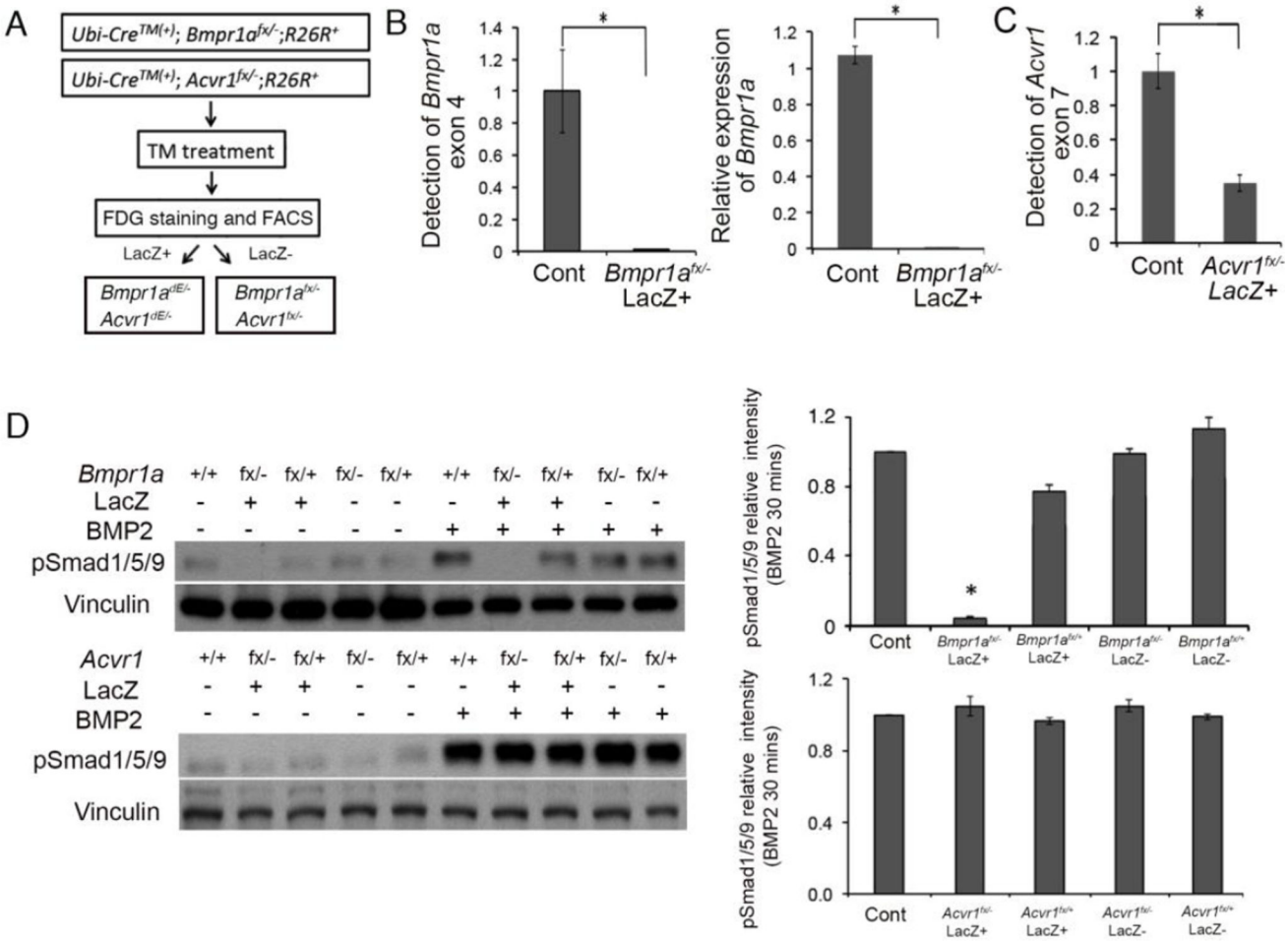

Fig. 6.

Bmpr1a, but not Acvr1 played important role in activating BMP signaling in pre-osteoblast. (A) Workflow of collecting Bmpr1a$^{dE/-}$ or Acvr1$^{dE/-}$ cells. Pre-osteoblasts isolated from calvaria of Ubi-Cre^{ERT2};Bmpr1a$^{fx/-}$, and Ubi-Cre^{ERT2}; Acvr1$^{fx/-}$, then treated with tamoxifen for 6 days. Cells were stained with FDG to separate lacZ(+) and lacZ(−) fractions. Cre-recombined homozygous null cells (Bmpr1a$^{dE/-}$ and Acvr1$^{dE/-}$) should be enriched in the lacZ(+) fractions. (B) Deletion of Bmpr1a exon 4 measured by genomic qPCR and expression levels of Bmpr1a measured by qRT-PCR. (C) Schemes of expected AcvrI wt and fx, Acvr1 null and Acvr1 dE exon structures and resulted sizes of PCR products. RT-PCR for a series samples indicated successful deletion of Acvr1 in cells after enrichment of LacZ expressing cells. LacZ in figure indicated sorted populations. To get Acvr1$^{-/-}$ DNA and RNA, intercross of Acvr1$^{+/-}$ mice was set up and embryos were isolated at E7.5 because of their lethality. (C right) Deletion of Acvr1 exon 7 measured by genomic qPCR. (D) Levels of Phospho-Smad1/5/9 (pSmad1/5/9) were examined in different cells with Bmpr1a mutant and Acvr1 mutant cells. Western blot results were quantified by densitometry (Image J). *, $p<0.05$.

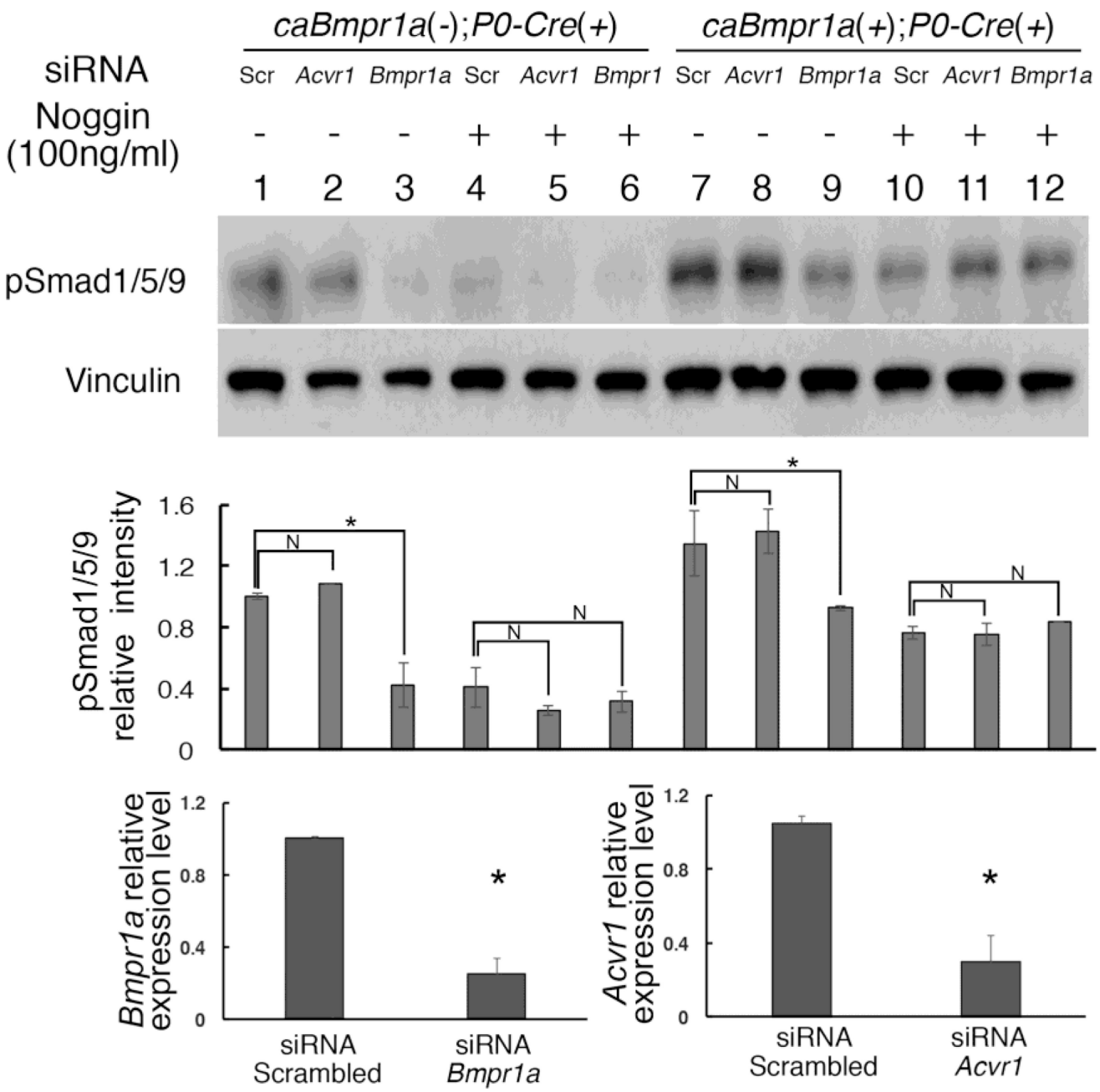

Fig. 7.

caBMPR1A did not require specific endogenous type 1 receptors for its BMP-Smad signaling. Calvarial preosteoblasts were prepared from control (caBmpr1a(−);P0-Cre(+)) and mutant (caBmpr1a(+);P0-Cre(+)) mice, and expression of endogenous type 1 receptors were reduced by siRNA for Bmpr1a or Acvr1. Cells were treated by Noggin to block ligand-dependent BMP signaling to visualize BMP-Smad signaling transduced only by caBMPR1A. Vinculin was used for loading control. Levels of gene silencing in the mutant cells were measured by Q-RT-PCR. Scr, scrambled, *, $p<0.01$, N, not significant.